Stability Analysis and Modeling of Fractional Chemical Reactions Model with Convergence Solutions

Muhammad Farman[1,2,3,*]*, H. M. Younas*[4]*, Ayesha Mukhtar*[4]*, Aseel Smerat*[5,6]*, Zaheer Ahmad*[7]*, and Mohamed Hafez*[8,9]

[1] Department of Mathematics, Faculty of Arts and Sciences, Near East University, PC: 99138, Nicosia /Mersin 10 – Turkey

[2] International Centre for Interdisciplinary Research in Sciences, The University of Lahore, 54100, Lahore, Pakistan

[3] Research Center of Applied Mathematics, Khazar University, Baku, AZ1096, Azerbaijan

[4] RIPHAH International University Faisalabad, Pakistan

[5] Faculty of Educational Sciences, Al-Ahliyya Amman University, Amman 19328, Jordan

[6] Department of Biosciences, Saveetha School of Engineering, Saveetha Institute of Medical and Technical Sciences, Chennai, 602105, India

[7] Institute of Mathematics, Khwaja Fareed University of Engineering and Information Technology, Raheem Yar Khan, Pakistan

[8] Faculty of Engineering and Quantity Surviving, INTI International University Colleges, Nilai, Malaysia

[9] Faculty of Management, Shinawatra University, PathumThani, 12000, Thailand

Abstract: The Brusselator system frequently emerges in the mathematical modeling of chemical reaction experiments. This study investigates the dynamic behavior of the Brusselator reaction model through the lens of the fractional Caputo derivative. The research focuses on analyzing the stability and dynamic properties of the associated fractional-order Brusselator system. Numerical examples are included to demonstrate the method's validity and efficiency.

1 Introduction, Motivation and Preliminaries

Recently, fractional calculus, involving both fractional derivatives and integrals, has garnered increasing interest across multiple scientific and engineering domains owing to its broad spectrum of applications [1,2,3,4]. Notable works such as quantum Lévy Processes and fractional market dynamics by Bulgac and Dang [5,6], and fractional-order state equations for control of viscoelastic structures by Calico [7], highlight its growing significance. Concurrently, chaos theory has emerged as a vital tool for analyzing the complex dynamics of differential systems. This has sparked growing interest in exploring chaotic phenomena within the framework of fractional dynamic systems. Fractional derivatives, known for their inherent memory and hereditary properties, offer a more accurate modeling framework for many real-world processes compared to traditional integer-order systems. Research indicates that systems exhibiting chaos in their classical forms often retain this behavior when reformulated using fractional-order derivatives [8,9]. For example, research works like chaos, control, and synchronization of a novel system and a chemical reactor system with function projective synchronization under parametric uncertainty highlight this trend consistently [10,11]. Further examples include investigations into exact solutions of diffusive predator-prey systems, Stochastic resonance in fractional linear oscillators, double-delay terms Robbin boundary value problem and fractional-order chuas System [12,13,14].

During the last thirty years, many fractional-order systems have been shown to display chaotic dynamics. Among these are fractional analogs of well-known chaotic systems like Chua, Lorenz, Chen, Arneodo, and the delayed Bloch system [15,16]. Ongoing research efforts focusing on areas such as chaotic dynamics and synchronization in Arneodo systems, nonlinear Bloch equations, discrete chaos in fractional delayed logistic models, and the presence of chaos and hyperchaos in fractional R'Osler equations are contributing significantly to the growth of this field [17,18,19].Chaotic

---

* Corresponding author e-mail: farmanlink@gmail.com

dynamics in fractional-order systems have also been identified in models such as the NewtonLeipnik system, as well as in investigations involving chemical instabilities and relaxation oscillations [20, 21]. In addition to classical integer-order systems, fractional-order dynamical systems governed by fractional differential equations have been widely studied, particularly in the context of biological and chemical reaction mechanisms [22, 23]. Researchers from the Brussels school have extensively explored the nonlinear oscillatory behavior of chemical reaction models [24]. Their investigations include foundational work on dissipative structures, chemical instabilities, and sustained oscillations in reaction systems. More recently, this line of inquiry has been extended to incorporate fractional-order modeling, as seen in studies on a fractional version of the dynamical Brusselator reaction-diffusion system [25].

$$\eta \to U$$
$$\omega + U \to V + P$$
$$2U + V \to 3U$$
$$U \to Q$$
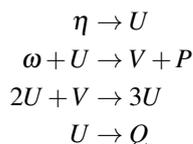
In the Brusselator model, the variables U and V denote intermediate species, while η and ω serve as reactants, and P and Q represent the final products. The concentrations of the intermediates are expressed as $u(x,t)$ and $v(x,t)$ respectively. It is generally assumed that the concentrations of the reactants η and ω remain constant throughout the reaction process. This reaction-diffusion system is particularly valuable for analyzing cooperative phenomena in chemical kinetics, with applications spanning enzymatic processes, plasma and laser dynamics, coupled reaction systems, and interactions involving ozone and atomic oxygen through triple collisions [26]. Further studies have examined the dynamic behavior of the Brusselator under impulsive inputs and strategies for controlling chaotic behavior in forced chemical reactions [27].

The dynamics of the system are:

$$\begin{cases} \dot{u}(x,y,t) = \eta + u^2 v - (\omega + 1)u, \\ \dot{v}(x,y,t) = -u^2 v + \omega u, \end{cases} \tag{1}$$

Subject to the IC's

$$(u(x,y,0), v(x,y,0)) = (g_1(x,y), g_2(x,y)) \tag{2}$$

In this scenario, $g_1(x,y)$ and $g_2(x,y)$ are defined functions, where x, y, and t act as the independent variables related to space and time. The constants ω and η represent the steady concentrations of the two reactants.

The fractional Brusselator system, expressed as a time-fractional system of differential equations, is derived by replacing the integer-order derivative with the Caputo fractional derivative.

$$\begin{cases} {}^C D_{0,t}^{\alpha} u(x,y,t) = \eta + u^2 v - (\omega + 1)u, \\ {}^C D_{0,t}^{\beta} v(x,y,t) = -u^2 v + \omega u, \end{cases} \tag{3}$$

Here, $0 < \alpha, \beta \leq 1$, and ${}^C D_{0,t}^{\alpha}$ and ${}^C D_{0,t}^{\beta}$ denote the fractional derivatives in the Caputo sense. If α is equal to β, the system represented by equation (**??**) is referred to as the comparable fractional-order Brusselator system; otherwise, it is considered a non-comparable system. Fractional differential equations (FDEs) have garnered significant attention, prompting the development of numerous analytical and numerical solution techniques [28]. Sarwar et al. [29], along with studies on the exact solutions of the nonlinear fractional Klein-Gordon equation using the optimal homotopy asymptotic method [30], contributed to extending the homotopy perturbation method (HPM) for solving fractional-order problems. Maryam et al. [31] utilized the method of lines to investigate the two-dimensional Brusselator system. Additionally, Hasib et al. [32] applied Bernstein polynomials for numerical solutions of the fractional-order Brusselator system, while Jafri et al. [33] focused on implementing HPM for the same model.

2 Preliminaries

Fractional calculus: This section provides an overview of fundamental definitions from the theory of fractional calculus [1, 3].

Definition 2.1. The non-integer integral ($\alpha > 0$) of $f \in C_\mu$, where $\mu \geq -1$, is expressed in the Riemann–Liouville framework as follows:

$$^{RL}D_{a,t}^{-\alpha} f(t) = \frac{1}{\Gamma(\alpha)} \int_a^t (t - \mu)^{\alpha - 1} f(\mu)\, d\mu, \qquad \alpha > 0,\ t > 0. \tag{4}$$

Definition 2.2. In the Riemann–Liouville framework, the fractional derivative of a function $f(t)$ of order α is defined as follows:

$$^{RL}D_{a,t}^{\alpha}f(t) = \frac{1}{\Gamma(n-\alpha)}\frac{d^n}{dt^n}\int_a^t (t-\mu)^{n-\alpha-1}f(\mu)\,d\mu, \quad \alpha > 0,\, t > 0, \tag{5}$$

where $n-1 < \alpha < n, n \in \mathbb{Z}^+$.

Definition 2.3. In the Caputo sense, the α-order derivative for $f \in C_{-1}^m$ is defined as:

$$^{C}D_{a,t}^{\alpha}f(x) = \frac{1}{\Gamma(m-\alpha)}\int_0^x (x-\eta)^{m-\alpha-1}f^{(m)}(\eta)\,d\eta, \tag{6}$$

where $m-1 < \alpha \le m, m \in \mathbb{Z}^+$.

Proposition 2.4. If $m-1 < \alpha \le m, m \in \mathbb{N}$, and $f \in C_\mu^m, \mu \ge -1$, then

$$^{RL}D_{a,t}^{-\alpha}\left(^{C}D_a^{\alpha}f(x)\right) = f(x) - \sum_{k=0}^{m-1}\frac{f^{(k)}(a)(x-a)^k}{\Gamma(k+1)}, \quad x > 0. \tag{7}$$

Lemma 2.5. Consider the following initial value problem (IVP):

$$\begin{cases} ^{C}D_{0,t}^{\alpha}x(t) = Ax(t) + F_1(x(t),y(t)), \\ ^{C}D_{0,t}^{\beta}y(t) = By(t) + F_2(x(t),y(t)), \end{cases} \tag{8}$$

If $x(t)$ and $y(t)$ are continuous functions, then the solutions $\psi_t(x,y) = (x(t),y(t))$ of system (8) can be written as:

$$\begin{cases} x(t) = x_0 E_{\alpha,1}(At^{\alpha}) + \int_0^t (t-\xi)^{\alpha-1}E_{\alpha,\alpha}(A(t-\xi)^{\alpha})F_1(x(\xi),y(\xi))\,d\xi, \\ y(t) = y_0 E_{\beta,1}(Bt^{\beta}) + \int_0^t (t-\xi)^{\beta-1}E_{\beta,\beta}(B(t-\xi)^{\beta})F_2(x(\xi),y(\xi))\,d\xi, \end{cases} \tag{9}$$

where $0 < \alpha, \beta < 1$ and x_0, y_0 are the initial conditions. $E_{\alpha,\beta}$ is the Mittag–Leffler function of two parameters, defined as:

$$E_{\alpha,\beta}(w) = \sum_{k=0}^{\infty}\frac{w^k}{\Gamma(k\alpha+\beta)}, \quad \alpha > 0,\, \beta \in \mathbb{R}. \tag{10}$$

3 Model Formulation and Geometric Interpretation

Phase Space Structure:
The system can be analyzed by studying trajectories in the (u,v)-plane at each spatial point. The interaction terms u^2v and ωu imply nonlinear coupling between the two variables. The behavior of the system is strongly influenced by the nonlinear term u^2v, which drives the autocatalytic feedback.

Fixed Points and Stability:
Points where $\dot{u} = \dot{v} = 0$ define the steady states (equilibria) of the system. By linearizing around these points, one can determine their stability, identifying whether solutions nearby converge, oscillate, or diverge â shaping the dynamical geometry of the system.

Nullclines and Flow Direction:
Curves where $\dot{u} = 0$ or $\dot{v} = 0$ can be used to dissect the vector field in phase space. These nullclines divide regions of different dynamical behavior and help visualize how solutions evolve over time.

Chemical Interpretation:
The term u^2v suggests a quadratic autocatalytic reaction, where the production of u depends on its own concentration and that of v. The loss terms like $(\omega+1)u$ and gain terms like ωu reflect natural decay or replenishment mechanisms.

Reaction Dynamics:
Depending on the parameters η and ω, and the initial conditions, the system may exhibit:

–Convergence to a stable chemical steady state

–Transient oscillations

–Describe the behavioof the Brusselator system when $\eta = 1$ and $\omega = 1$.

4 HPM Algorithm for a Chemical Reactions Model

Suppose the governing model is a system of nonlinear chemical reaction partial differential equations of the form:

$$L(u) + N(u) = f(t), \quad u(0) = u_0, \tag{10}$$

where L is a linear operator, N is a nonlinear operator (e.g., reaction terms like u^2, uv), $f(t)$ is a source/input term (may represent inflow/outflow rates or catalysts), and $u(t)$ is the concentration(s) of species.

Step 1: Construct Homotopy

Build the homotopy equation with an embedding parameter $p \in [0,1]$:

$$H(u,p) = (1-p)[L(u) + N(u)] + p[L(u) + N(u) - f(t)] = 0 \tag{11}$$

–When $p = 0$, $H(u,0) = 0 \implies u = u_0$ (initial approximation).

–When $p = 1$, $H(u,1) = 0 \implies$ original chemical reaction model.

Step 2: Assume Perturbation Expansion

Assume the solution can be expanded in powers of p:

$$u = u_0 + pu_1 + p^2 u_2 + p^3 u_3 + \dots \tag{12}$$

Step 3: Substitute into Homotopy

Insert the expansion into the homotopy $H(u,p) = 0$.

Step 4: Equating Coefficients

Collect terms of like powers of p:

–p^0: Gives the zeroth-order problem (usually a linear ODE/PDE).

–p^1: Gives the first-order correction equation.

–p^2: Gives the second-order correction equation, and so on.

Each equation is typically linear and easier to solve than the full nonlinear model.

Step 5: Iterative Solutions

Solve sequentially:

$$u_0 \to u_1, \quad u_1 \to u_2, \quad \dots$$

Step 6: Construct Approximate Solution

Finally, set $p = 1$ to obtain the approximate solution:

5 Convergence Analysis of Applications

Definition 5.1. The Fractional Time Homotopy Perturbation Method (HPM) is applied to differential equations, especially those involving fractional calculus. Once an approximation of a solution is determined, one can measure how close it is to the exact solution. This brings along an important notion: **Absolute Error**.

Absolute Error Theorem

Let $u(t)$ denote the exact solution to a fractional differential equation, and let $u_n(t)$ be the approximate solution obtained by the n-th order approximation of HPM. Then, the absolute error $E_n(t)$ is defined as

$$E_n(t) = |u(t) - u_n(t)|, \tag{13}$$

and as $n \to \infty$, the approximate solution converges to the exact solution:

$$\lim_{n\to\infty} E_n(t) = 0, \quad \forall t. \tag{14}$$

This guarantees that the absolute difference between the exact and approximate solution decreases as more perturbation terms are considered. Higher-order approximations provide more accurate solutions.

Definition 5.2. The **Relative Error** of HPM is a measure of the error magnitude relative to the exact solution. Let $u(t)$ be the exact solution and $u_n(t)$ the n-th order approximate solution. Then the relative error $R_n(t)$ is defined as

$$R_n(t) = \frac{|u(t) - u_n(t)|}{|u(t)|}, \tag{15}$$

and as $n \to \infty$,

$$\lim_{n\to\infty} R_n(t) = 0, \quad \forall t \text{ where } u(t) \neq 0. \tag{16}$$

Definition 5.3. The L_2**-norm** measures the "average" error over a time interval $[a,b]$. For the n-th order HPM approximation $u_n(t)$ of the exact solution $u(t)$, the L_2-norm of the error is

$$\|E_n(t)\|_2 = \left(\int_a^b \left(u(t) - u_n(t) \right)^2 dt \right)^{1/2}. \tag{17}$$

As $n \to \infty$,

$$\lim_{n\to\infty} \|E_n(t)\|_2 = 0, \tag{18}$$

indicating convergence in the L_2-sense.

Definition 5.4. The L_∞**-norm** measures the maximum error over a time interval $[a,b]$. For $u_n(t)$ approximating $u(t)$, it is defined as

$$\|E_n(t)\|_\infty = \max_{t\in[a,b]} |u(t) - u_n(t)|. \tag{19}$$

As $n \to \infty$,

$$\lim_{n\to\infty} \|E_n(t)\|_\infty = 0, \tag{20}$$

ensuring that the maximum error decreases as more perturbation terms are included, proving convergence in the L_∞-sense. This theorem ensures that any increase in the number of perturbation terms results in a decrease of the maximum error between the exact and approximate solutions; thus, the theorem proves convergence of the approximation in the L_∞-sense.

6 Analysis of Stability in Nonlinear Fractional Dynamic Systems

This section provides the stability theorem and stability analysis of the chemical reactions, specifically the Brusselator system with fractional order. Examine the nonlinear fractional dynamical system described as:

$$
\begin{cases}
{}^{C}D_{0,t}^{\gamma_1} x_1 = f_1(x_1, x_2, \ldots, x_n), \\
{}^{C}D_{0,t}^{\gamma_2} x_2 = f_2(x_1, x_2, \ldots, x_n), \\
\vdots \\
{}^{C}D_{0,t}^{\gamma_n} x_n = f_n(x_1, x_2, \ldots, x_n),
\end{cases}
\tag{21}
$$

where $\gamma_1 = \gamma_2 = \cdots = \gamma_n = \gamma$, system (21) is referred to as a *comparable fractional dynamical system*. Otherwise, it is an *unequal fractional dynamical system*.

The equilibrium points $E^* = (x_1^*, x_2^*, \ldots, x_n^*)$ are determined by solving:

$$
\begin{cases}
f_1(x_1, x_2, \ldots, x_n) = 0, \\
f_2(x_1, x_2, \ldots, x_n) = 0, \\
\vdots \\
f_n(x_1, x_2, \ldots, x_n) = 0,
\end{cases}
\tag{22}
$$

Theorem 6.1. A fractional dynamical system (23) is considered asymptotically stable for $\gamma_1 = \gamma_2 = \cdots = \gamma_n = \gamma$ if all eigenvalues λ_i, $(i = 1, 2, \ldots, n)$ of the Jacobian matrix

$$
J = \frac{\partial f}{\partial x} \bigg|_{E^*}, \quad f = [f_1, f_2, \ldots, f_n]^T
\tag{23}
$$

satisfy the condition:

$$
|\arg(\lambda_i)| > \frac{\gamma \pi}{2}, \quad \forall i = 1, 2, \ldots, n.
\tag{24}
$$

6.1 Study of Nonlinear Brusselator Dynamics under Fractional Calculus

This section discusses the local stability and dynamic behavior of the nonlinear fractional Brusselator system.

The equilibrium point $E^* = (\eta, \omega/\eta)$ of system (**??**) is determined by solving:

$$
\eta + u^2 v - (\omega + 1)u = 0, \quad -u^2 v + \omega u = 0
$$

The Jacobian matrix J at $E^* = (\eta, \omega/\eta)$ is:

$$
J = \begin{pmatrix} \omega - 1 & \eta^2 \\ -\omega & -\eta^2 \end{pmatrix}
\tag{25}
$$

The associated characteristic equation is:

$$
\lambda^2 + \lambda(\eta^2 - \omega + 1) + \eta^2 = 0
\tag{26}
$$

Selecting fractional derivative orders as $\gamma = \alpha = \beta = 0.97$ and setting $\eta = 1$ and $\omega = 2.25$, the computed eigenvalues are:

$$
\lambda_{1,2} = 0.125 \pm 0.9921i
$$

Consequently,

$$
|\arg(\lambda_1 \text{ or } \lambda_2)| \approx 1.4454 < 0.97\frac{\pi}{2} \approx 1.5236
$$

To study the dynamic behavior of the fractional Brusselator system, the parameters $\eta = 1$ and $\omega = 2.25$ are held fixed, and the fractional order γ is gradually varied from 0.65 to 1 with a step size of 0.01. The Lyapunov exponents λ_{LE_1} and

λ_{LE_2} of system (**??**) are negative. Thus, system (**??**) exhibits multiple negative Lyapunov exponents at different fractional orders γ. For instance, for $\gamma = 0.95$:

$$\lambda_{LE_1} = -0.0089, \quad \lambda_{LE_2} = -0.4318$$

and for $\gamma = 0.97$:

$$\lambda_{LE_1} = -0.0076, \quad \lambda_{LE_2} = -0.3817$$

indicating that the system's orbit converges to a stable periodic orbit. According to Routh's theorem [**?**], the characteristic equation (26) suggests that the system is unstable near the fixed point if and only if

$$\omega > \eta^2 + 1,$$

while stability is ensured when

$$\omega < \eta^2 + 1.$$

6.2 Formulation of Fractional Brusselator System with Diffusion

The implementation of the HPM algorithm for the fractional-order Brusselator system (**??**), including diffusion, is presented below.

The fractional system with diffusion can be expressed as:

$$\begin{cases} {}^cD_t^\alpha u(r,t) - \eta - u^2 v + (\omega+1)u - \delta\nabla u = 0, \\ {}^cD_t^\beta v(r,t) + u^2 v - \omega u - \delta\nabla v = 0, \end{cases} \tag{27}$$

subject to the initial condition:

$$(u(r,0), v(r,0)) = (g_1(r), g_2(r)). \tag{28}$$

Here, $u(r,t)$ and $v(r,t)$ are unknown functions depending on the spatial variable r and temporal variable t, ∇ is the two-dimensional Laplace operator, and δ is the diffusion coefficient.

6.2.1 Homotopy Construction

Construct the homotopy for the system as

$$\phi_1(r,t;p) : \Omega \times [0,1] \to \mathbb{R}, \quad \phi_2(r,t;p) : \Psi \times [0,1] \to \mathbb{R},$$

such that

$$\begin{cases} (1-p)\,{}^cD_{0,t}^\alpha \phi_1(r,t) + p\left[{}^cD_{0,t}^\alpha \phi_1 - \phi_1^2\phi_2 + (\omega+1)\phi_1 - \delta\nabla\phi_1 - \eta\right] = 0, \\ (1-p)\,{}^cD_{0,t}^\beta \phi_2(r,t) + p\left[{}^cD_{0,t}^\beta \phi_2 - \phi_1^2\phi_2 - \omega\phi_1 - \delta\nabla\phi_2\right] = 0, \end{cases} \tag{29}$$

where $p \in [0,1]$ is the embedding parameter, and $H_1(p), H_2(p)$ are non-zero functions.

6.2.2 Series Expansion of Solutions

Assume the solutions $\phi_1(r,t;p)$ and $\phi_2(r,t;p)$ can be expanded in powers of p as:

$$\begin{cases} \phi_1(r,t;p) = u_0(r,t) + \sum_{k=1}^m u_k(r,t)\,p^k, \\ \phi_2(r,t;p) = v_0(r,t) + \sum_{k=1}^m v_k(r,t)\,p^k, \end{cases} \tag{30}$$

for $i = 1,2,\ldots,m$, where $u_0(r,t)$ and $v_0(r,t)$ are the initial approximations.

6.2.3 Remark

It has been noted that the convergence of system (32) is influenced by the parameters controlling convergence. If it converges at $p = 1$, one can write:

$$\begin{cases} u(r,t) = u_0(r,t) + \sum_{k=1}^{m} u_k(r,t), \\ v(r,t) = v_0(r,t) + \sum_{k=1}^{m} v_k(r,t). \end{cases} \tag{31}$$

By substituting system (30) into system (31) and equating coefficients of corresponding powers of p, the zeroth, first, second, and higher-order systems can be obtained.

6.2.4 Application of Brusselator System in Chemical Reactions

The procedure for employing HPM to solve the fractional-order Brusselator model with diffusion is as follows:

Governing System in Fractional Form

$$\begin{cases} {}^cD_{0,t}^{\alpha} u(x,y,t) = u^2 v - 2u + \frac{1}{4}\left(\frac{\partial^2 u}{\partial x^2} + \frac{\partial^2 u}{\partial y^2}\right), \\ {}^cD_{0,t}^{\beta} v(x,y,t) = u - u^2 v + \frac{1}{4}\left(\frac{\partial^2 v}{\partial x^2} + \frac{\partial^2 v}{\partial y^2}\right), \end{cases} \quad 0 < \alpha, \beta < 1. \tag{32}$$

Initial Conditions

$$u(x,y,0) = e^{-x-y}, \quad v(x,y,0) = e^{x+y}. \tag{33}$$

Exact Solutions

$$u(x,y,t) = e^{-x-y-1/2}, \quad v(x,y,t) = e^{-x-y+1/2}. \tag{34}$$

Homotopy Perturbation Series

$$p^0: \quad u_0 = e^{-x-y}, \quad v_0 = e^{x+y},$$

$$p^1: \quad \begin{cases} {}^cD_t^{\alpha} u_1 - u_0^2 v_0 + 2u_0 - \frac{1}{4}(u_{0,xx} + u_{0,yy}) = 0, \\ {}^cD_t^{\alpha} v_1 - u_0 - u_0^2 v_0 - \frac{1}{4}(v_{0,xx} + v_{0,yy}) = 0 \end{cases}$$

$$p^2: \quad \begin{cases} {}^cD_t^{\alpha} u_2 - u_0^2 v_1 - 2u_0 u_1 v_0 + 2u_1 - \frac{1}{4}(u_{1,xx} + u_{1,yy}) = 0, \\ {}^cD_t^{\alpha} v_2 - u_1 + u_0^2 v_1 + 2u_0 u_1 v_0 - \frac{1}{4}(v_{1,xx} + v_{1,yy}) = 0 \end{cases}$$

Zeroth-, First-, and Second-Order Solutions

$$u_0(x,y,t) = e^{-x-y}, \quad v_0(x,y,t) = e^{x+y}. \tag{35}$$

$$u_1 = -\frac{1}{2\Gamma(1+\alpha)} e^{-x-y} t^{\alpha}, \quad v_1 = \frac{1}{2\Gamma(1+\beta)} e^{x+y} t^{\beta}. \tag{36}$$

$$\begin{cases} u_2 = \frac{1}{2\Gamma(2\beta+1)} e^{-x-y} t^{2\beta} - \frac{1}{\Gamma(2\alpha+1)} e^{-x-y} t^{2\alpha}, \\ v_2 = \frac{1}{2\Gamma(2\alpha+1)} e^{-x-y} t^{2\alpha} + \frac{1}{4\Gamma(2\beta+1)} e^{x+y} t^{2\beta} - \frac{1}{2\Gamma(1+2\beta)} e^{-x-y} t^{2\beta}. \end{cases} \tag{37}$$

Approximate Solutions Substituting the above results, the approximate solutions can be written as:

$$\begin{cases} U = e^{-x-y} - \frac{1}{2\Gamma(1+\alpha)} e^{-x-y} t^{\alpha} - \frac{1}{4\Gamma(1+2\alpha)} e^{-x-y} t^{2\alpha} + \frac{1}{2\Gamma(1+2\beta)} e^{-x-y} t^{2\beta}, \\ V = e^{x+y} - \frac{1}{2\Gamma(1+2\alpha)} e^{-x-y} t^{2\alpha} + \frac{1}{2\Gamma(1+\beta)} e^{x+y} t^{\beta} - \frac{1}{2\Gamma(1+2\beta)} e^{-x-y} t^{2\beta} + \frac{1}{4\Gamma(1+2\beta)} e^{x+y} t^{2\beta}. \end{cases} \tag{38}$$

System (38) represents the parameter of convergence.

7 Results and Discussions with Comparison

Section 6 demonstrates the application of the extended Homotopy Perturbation Method (HPM) to the fractional Brusselator dynamical system with parameters $\mu = 1$, $\Omega = 0$, and $\delta = 0.25$. Highly accurate second-order solutions for $U(x,y,t)$ and $V(x,y,t)$ are provided in Eq. (37). These solutions are based on convergence control parameters, which are detailed in Table 1 for $U(x,y,t)$ and Table 2 for $V(x,y,t)$.

Specific values for the fractional orders α and β include:

$$\alpha = 0.5, \beta = 0.75; \quad \alpha = 0.75, \beta = 0.5; \quad \alpha = \beta = 1; \quad \alpha = 0.5, \beta = 0.75; \quad \alpha = 0.75, \beta = 0.65; \quad \alpha = \beta = 1,$$

respectively.

Tables 1 and 2 represent a comparison of the absolute errors for $U(x,y,t)$ and $V(x,y,t)$ at various grid points, highlighting the differences between the HPM results and the exact solutions, specifically for second-order approximations. As illustrated in Tables 3, 4, 5, and 6, the HPM delivers highly accurate outcomes at the second-order approximation level without the need for spatial discretization. This demonstrates that the second-order results of the fractional Brusselator reaction-diffusion system achieve efficient convergence.

Figures 1-2 represent the 2D fractional behavior of u and v of the Brusselator system at $t = 1$ for different values of α and β. Figures 5-6 show the 3D fractional surface behavior of u and v in the chemical reaction at $t = 1$, also for various values of α and β. Figures 7-8 illustrate the 2D approximate and exact behavior of the Brusselator system through contours, whereas Figures 9-10 represent the 3D visualization of approximate and exact solutions through contours. Figures 11-12 describe the error distribution in 2D and 3D. The figures clearly illustrate that the approximate solutions closely resemble the exact solution. These approximations converge efficiently, making the computation of additional terms unnecessary when applying the Homotopy Perturbation Method (HPM). The strong agreement between the approximate and exact solutions demonstrates the methodâs accuracy. Overall, the results confirm that HPM is highly effective in accurately solving fractional-order nonlinear partial differential equations with reduced computational effort.

Table 1: Assessment of the error distribution between HPM and the exact solution over successive terms for $U(x,y,t)$.

t	x	Relative Error	Absolute Error
0.25	0.25	3.5762×10^{-4}	1.9142×10^{-4}
		3.5762×10^{-4}	1.4908×10^{-4}
		3.5762×10^{-4}	1.1610×10^{-4}
	L2	9.7676×10^{-3}	
	L_∞	3.7899×10^{-3}	
0.5	0.5	3.1449×10^{-3}	1.1569×10^{-3}
		3.1449×10^{-3}	9.0102×10^{-4}
		3.1449×10^{-3}	7.0171×10^{-4}
	L2	1.6161×10^{-3}	
	L_∞	0.4079	
0.75	0.75	1.1674×10^{-2}	2.9516×10^{-3}
		1.1674×10^{-2}	2.2987×10^{-3}
		1.1674×10^{-2}	1.7902×10^{-3}
	L2	2.4919×10^{-2}	
	L_∞	1.6977	

Table 2: An error evaluation between the HPM solution and the exact solution across various terms for $V(x,y,t)$.

t	x	Relative Error	Absolute Error
0.25	0.25	2.8503	1.9266×10^{-1}
		5.3480	2.4737×10^{-1}
		9.4661	3.1764×10^{-1}
	L2	5.4713	
	L_∞	3.7899×10^{-3}	
0.5	0.5	7.6319	1.9266×10^{-1}
		13.2316	2.4737×10^{-1}
		22.4639	3.1764×10^{-1}
	L2	2.4955	
	L_∞	0.4079	
0.75	0.75	17.8143	1.9266×10^{-1}
		30.0195	2.4737×10^{-1}
		50.1425	3.1764×10^{-1}
	L2	6.4409	
	L_∞	1.6977	

Table 3: Fractional comparison between current results and OHAM for various values of α and β for $U(x,y,t)$.

t	x	y	U_1 (Current, $\alpha=0.5, \beta=0.75$)	U_1 (OHAM [40])	U_2 (Current, $\alpha=0.75, \beta=0.5$)	U_2 (OHAM [40])
0.25	0.25	0.25	0.42604	0.446432	0.518482	0.520062
		0.5	0.3318	0.347682	0.403794	0.405024
		0.75	0.258406	0.270775	0.314475	0.315433
0.5	0.5	0.25	0.287689	0.310039	0.370370	0.366170
		0.5	0.224053	0.241459	0.288444	0.285174
		0.75	0.174492	0.188048	0.224641	0.222094
0.75	0.75	0.25	0.209029	0.226141	0.270111	0.260696
		0.5	0.162792	0.176119	0.210363	0.203030
		0.75	0.126782	0.137162	0.163831	0.158120

Table 4: Classical comparison between current results, OHAM, and exact solutions for $U(x,y,t)$ with $\alpha=1$, $\beta=1$.

t	x	y	U_3 (Current)	U_3 (OHAM [40])	U_3 (Exact)
0.25	0.25	0.25	0.535453	0.535806	0.535261
		0.5	0.417011	0.417286	0.416862
		0.75	0.324769	0.324983	0.324652
0.5	0.5	0.25	0.369036	0.368810	0.367879
		0.5	0.287406	0.287230	0.286505
		0.75	0.223832	0.223695	0.223130
0.75	0.75	0.25	0.255791	0.254621	0.252840
		0.5	0.199210	0.198299	0.196912
		0.75	0.155145	0.154435	0.153355

Table 5: Fractional comparison between current results and OHAM for $V(x,y,t)$ with various values of α and β.

t	x	y	V_1 (Current, $\alpha = 0.5, \beta = 0.75$)	V_1 (OHAM [40])	V_2 (Current, $\alpha = 0.75, \beta = 0.65$)	V_2 (OHAM [40])
0.25	0.25	0.25	2.33740	2.23662	2.37244	2.00882
		0.5	2.97378	2.87188	3.05647	2.57938
		0.75	3.79699	3.68757	3.93252	3.31199
0.5	0.5	0.25	3.52227	3.29064	3.60142	2.97264
		0.5	4.50468	4.22527	4.63159	3.81695
		0.75	5.77010	5.42535	5.95275	4.90106
0.75	0.75	0.25	5.12040	4.69196	5.21495	4.32645
		0.5	6.56540	6.02460	6.70027	5.55527
		0.75	8.42288	7.73573	8.60655	7.13311

Table 6: Classical comparison between current results, OHAM, and exact solutions for $V(x,y,t)$ with $\alpha = 1, \beta = 1$.

t	x	y	V_3 (Current)	V_3 (OHAM [40])	V_3 (Exact)
0.25	0.25	0.25	2.06090	1.86783	1.86825
		0.5	2.64625	2.39834	2.39888
		0.75	3.39785	3.07953	3.08022
0.5	0.5	0.25	3.17550	2.71853	2.71828
		0.5	4.07742	3.49066	3.49034
		0.75	5.23551	4.48210	4.48169
0.75	0.75	0.25	4.75699	3.95169	3.95508
		0.5	6.10810	5.07408	5.07842
		0.75	7.84296	6.51524	6.52082
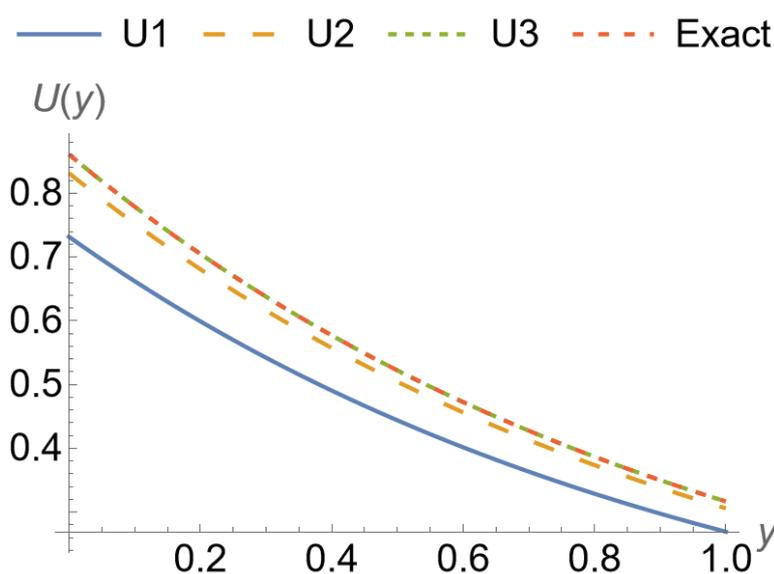
Fig. 1: Predicted results for $U(x,y,t)$
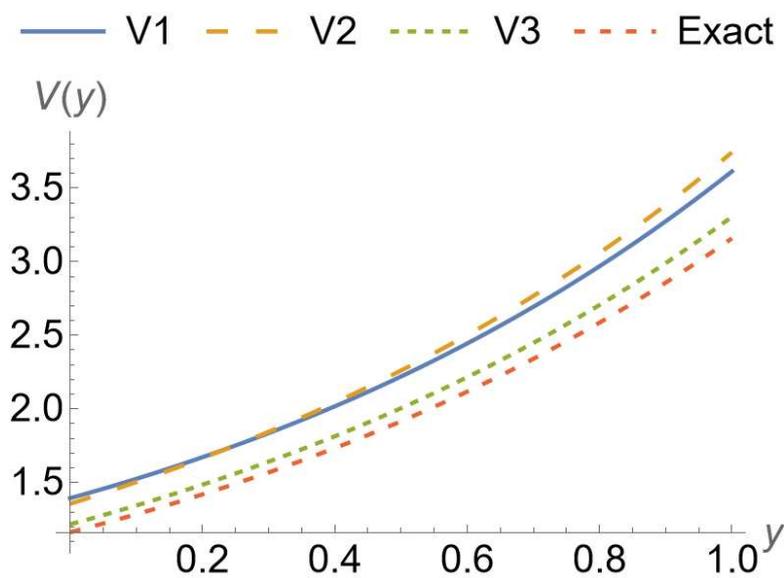
Fig. 2: Predicted results for $V(x,y,t)$
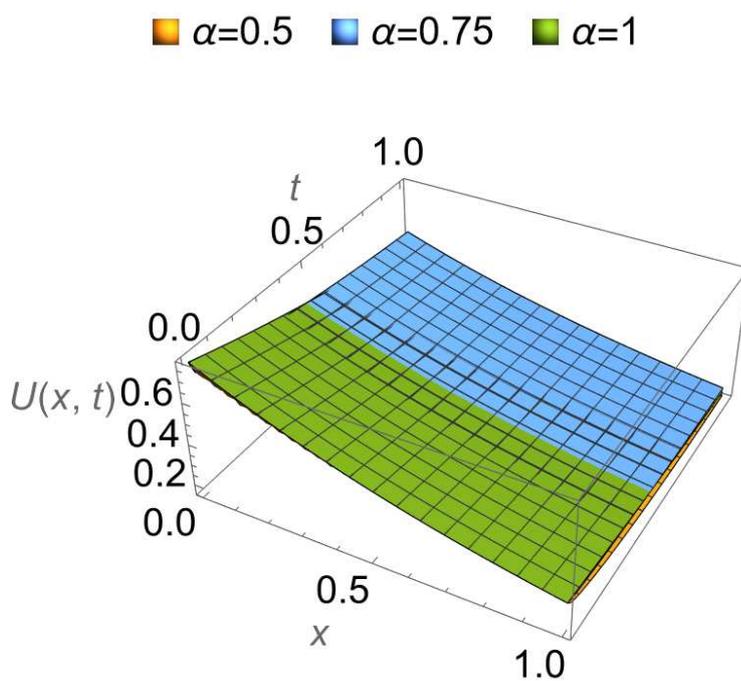
Fig. 3: Represent the convergence of $U(x,y,t)$ in 3D
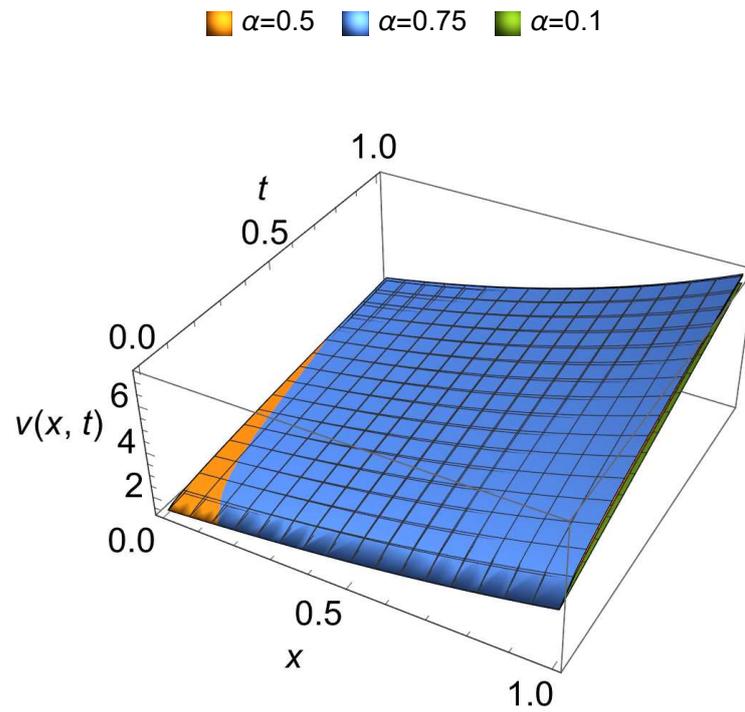
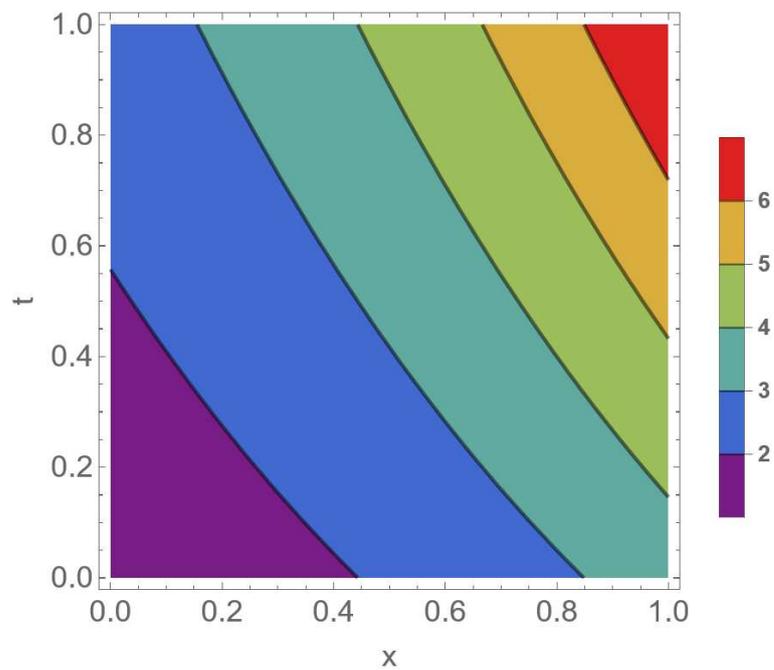**Fig. 4:** Represent the convergence of $V(x, y, t)$ in 3D

Fig. 5: Visualization of $U(x, t)$ Solutions Through Contours
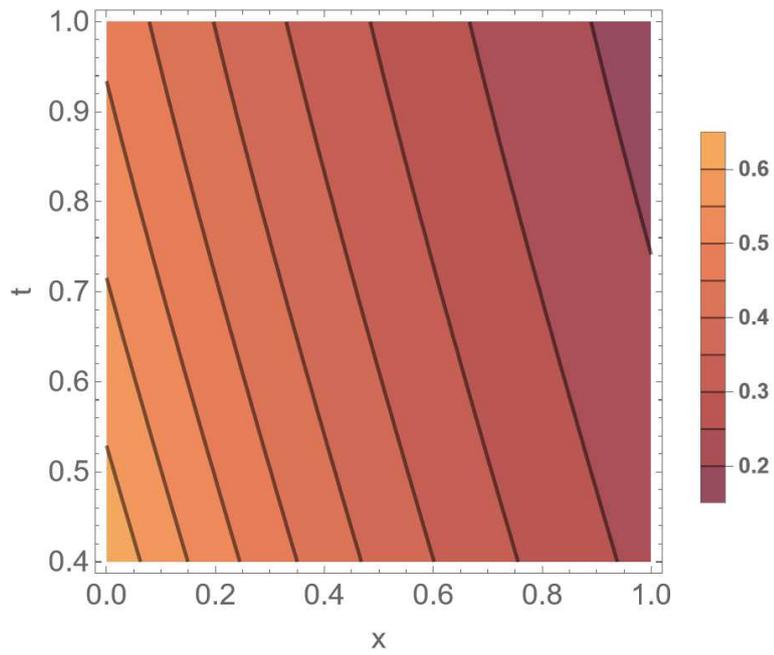
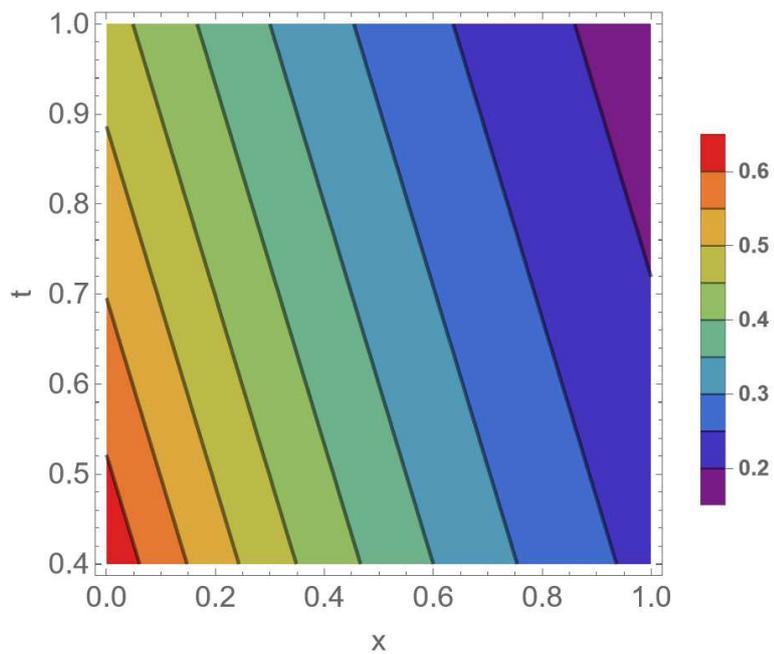**Fig. 6:** Contour plot of $V(x,t)$ Solutions
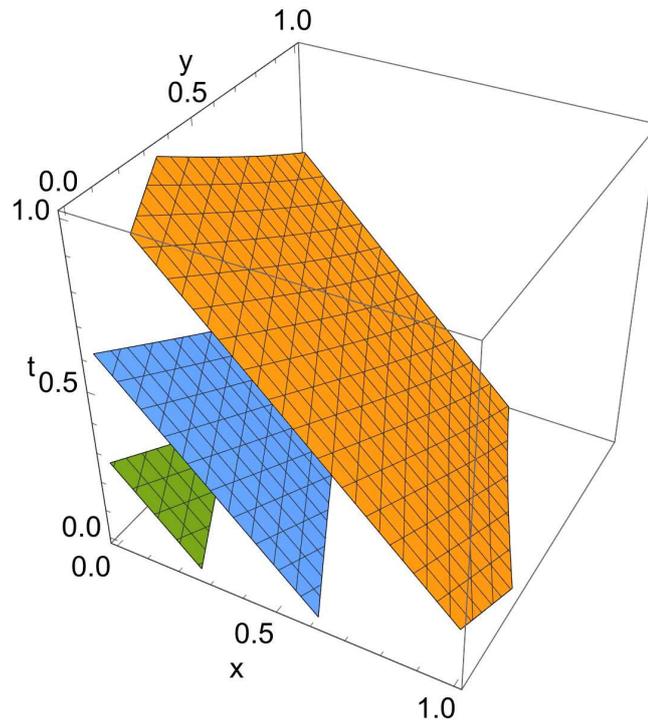

Fig. 7: Contour plot of the first exact solutions

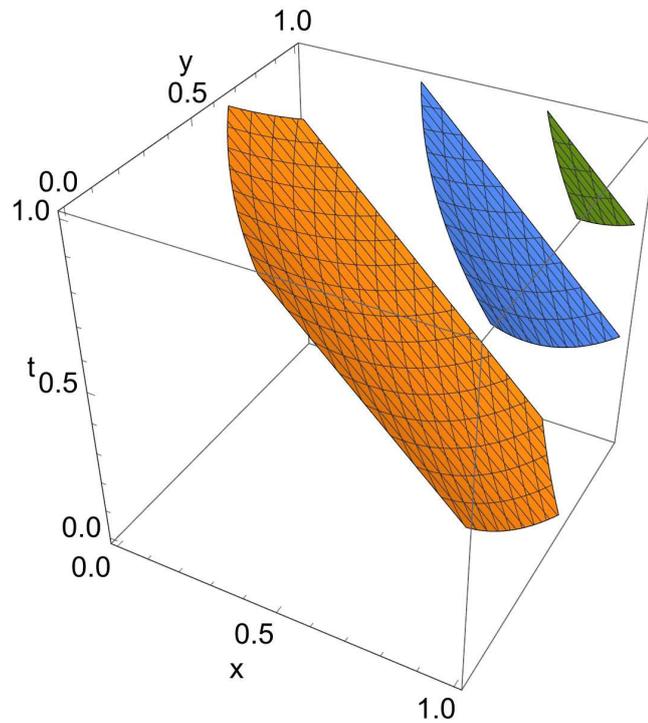**Fig. 8:** Visualization of Exact Solutions Through Contours
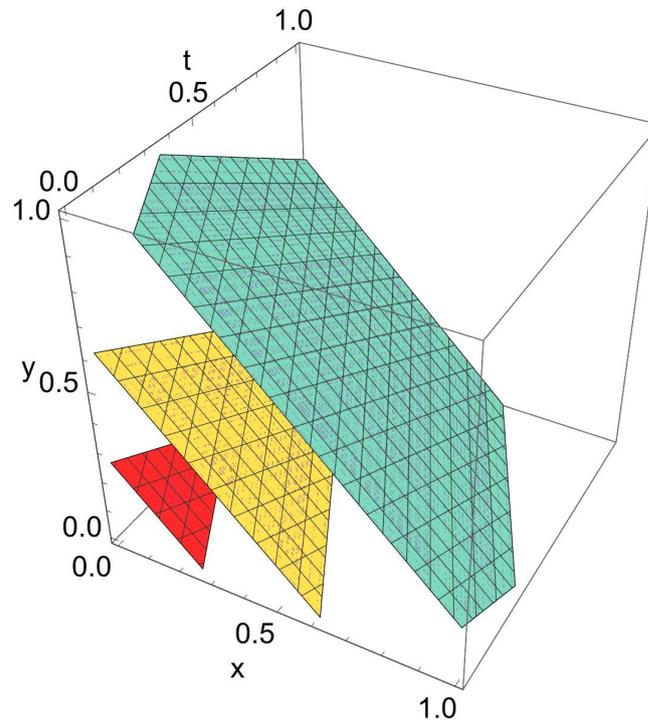

Fig. 9: 3D Contour Visualization of Approximate Solutions

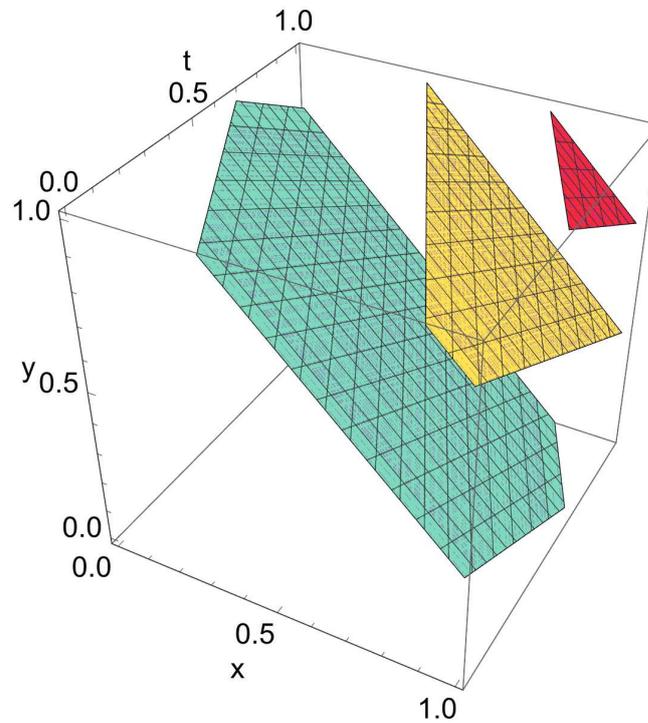**Fig. 10:** Contour-Based 3D Representation of the Approximate

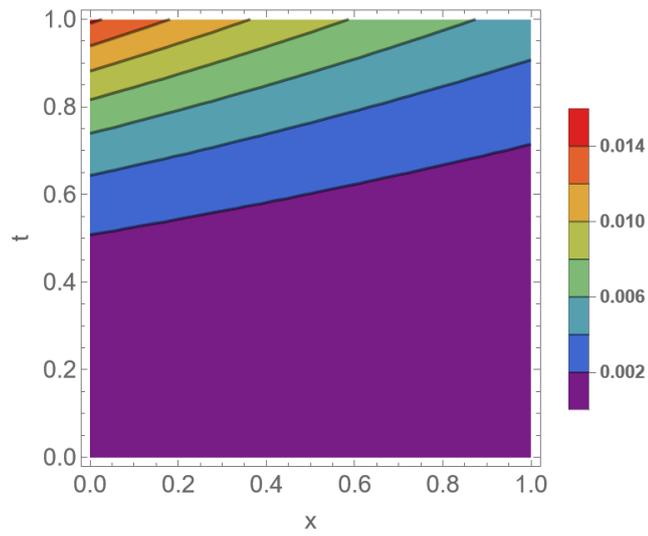**Fig. 11:** Contour-Based 3D Exact Solutions

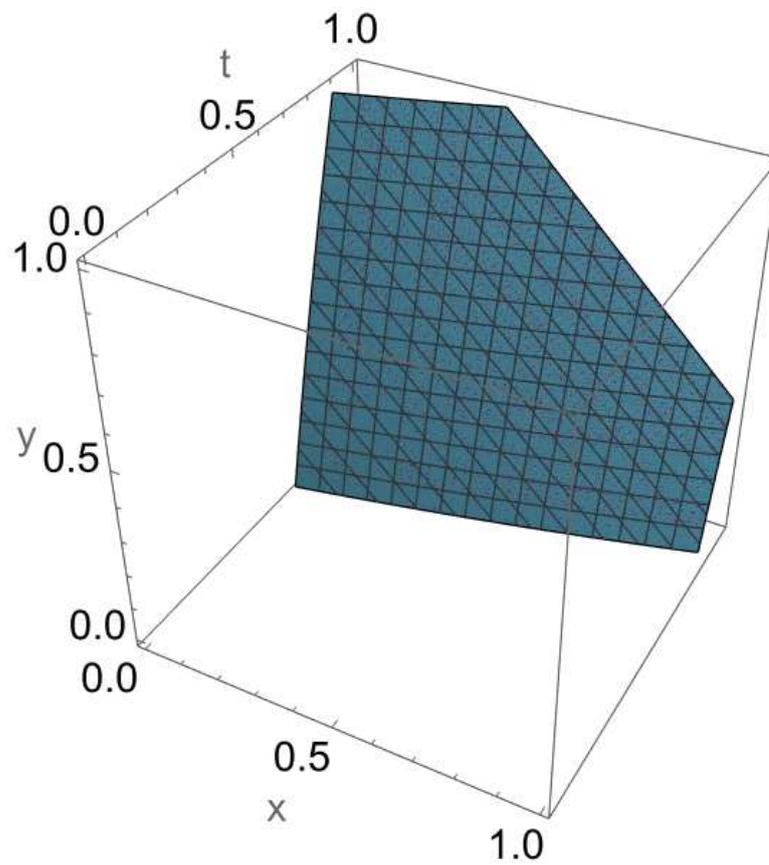**Fig. 12:** Contour-Based 2D Representation of error

Fig. 13: Contour-Based 3D Representation of error

8 Conclusion

This study explores the dynamics of a fractional-order Brusselator system, which originates from chemical reaction models and is described using the Caputo fractional derivative. Through analytical methods and numerical simulations, it was found that although the equilibrium point of the system is unstable, the system tends toward asymptotic stability as the order of the fractional derivative changes. The commensurate form of the system demonstrated both chaotic patterns and the presence of limit cycles. To address the fractional nonlinear Brusselator system with diffusion, the Homotopy Perturbation Method (HPM) was employed. Unlike conventional numerical methods that rely on discretization, HPM provides rapid convergence with minimal approximation levels. The research emphasized evaluating the convergence behavior and overall efficiency of HPM, concluding that it is a robust and effective technique for analyzing fractional-order systems across various scientific and engineering applications.

References

[1] Podlubny, *Fractional differential equations*, North-Holland Mathematical Studies, New York (NY): Academic Press (1999).

[2] A. Hussain, M. Hammad, A. A. Rahimzai, W. S. Koh, and I. Khan, Dynamical analysis and soliton solutions of the spacetime fractional Kaup-Boussinesq system. *Partial Differential Equations in Applied Mathematics*, 101205, (2025).

[3] C. P. Li, and F. H. Zeng, *Physics of Fractal Operators*, Springer, Berlin, Heidelberg and New York, (2003).

[4] S. Jamil, K. Jamil, and A. Shehzad, Modeling and Stability Analysis of the Unemployment Model with Caputo, *Journal of Mathematical Modeling and Fractional Calculus*, **1**(2), 23-39, (2025).

[5] D. Kusnezov, A. Bulgac and G.D. Dang, *Quantum Levy Processes and Fractional Kinetics*, Physical review letters, **82**(6) (1999).

[6] N. Laskin, *Fractional market dynamics*, Physica A: Statistical Mechanics and its Applications, **287**(3-4), 482-492, (2000).

[7] R. L. Bagley and R. A. Calico, Fractional order state equations for control of viscoelastic structures, *Journal of Guidance, Control, and Dynamics*, **14**(2), 304-311, (1991).

[8] I. Petras, *Fractional-order Nonlinear Systems: Modeling, Analysis and Simulation*, Springer, Heidelberg, (2011).

[9] K. Faiz, A. Ahmad, M. S. Khan, and S. Abbas, Control of Marburg Virus Disease Spread in Humans under Hypersensitive Response through Fractal-Fractional, *Journal of Mathematical Modeling and Fractional Calculus*, **1**(1), 88-113, (2024).

[10] K. Vishal and S. K. Agrawal, On the dynamics, existence of chaos control and synchronization of a novel complex chaotic system, *Chinese Journal of Physics*, **55**(2), 519-532, (2017).

[11] V. K. Yadav, S. Das, B. S. Bhadauria, A. K. Singh, and M. Srivastava, Stability analysis, chaos control of a fractional order chaotic chemical reactor system and its function projective synchronization with parametric uncertainties. *Chinese Journal of Physics*, **55**(3), 594-605, (2017).

[12] J. Choi, H. Kim, and R. Sakthivel, On certain exact solutions of diffusive predator-prey system of fractional order, *Chinese Journal of Physics*, **54**(1), 135-146, (2016).

[13] S. Ullah, A. Ullah, A. Ullah, and M. A. Mostafa, KhaterOn Double Delay Terms Robbin Boundary Value Problem with Fractional Derivative, *Journal of Mathematical Modeling and Fractional Calculus*, **1**(2), 88-106, (2025).

[14] Z. Q. Huang and F. Guo, Stochastic resonance in a fractional linear oscillator subject to random viscous damping and signal-modulated noise, *Chinese Journal of Physics* **54**(1), 69-76, (2016).

[15] T. T. Hartley, C. F. Lorenzo, and H. K. Qammer, Chaos in a fractional order Chua's system, *IEEE Transactions on Circuits and Systems I: Fundamental Theory and Applications*, **42**(8), 485-490, (1995).

[16] I. Grigorenko and E. Grigorenko, Chaotic dynamics of the fractional Lorenz system, *Physical review letters*, **91**(3), 034101, (2003).

[17] C. Li and G. Chen, Chaos in the fractional order Chen system and its control, *Chaos, Solitons & Fractals*, **22**(3), 549-554. (2004).

[18] D. Baleanu, R. L. Magin, S. Bhalekar, and V. Daftardar-Gejji, Chaos in the fractional order nonlinear Bloch equation with delay, *Communications in Nonlinear Science and Numerical Simulation*, **25**(1-3), 41-49, (2015).

[19] G. C. Wu and D. Baleanu, Discrete chaos in fractional delayed logistic maps, *Nonlinear Dynamics*, **80**(4), 1697-1703, (2015).

[20] C. Li, and G. Chen, Chaos and hyperchaos in the fractional-order Rössler equations, *Physica A: Statistical Mechanics and its Applications*, **341**, 55-61, (2004).

[21] L. J. Sheu, H. K. Chen, J. H. Chen, L. M. Tam, W. C. Chen, K. T. Lin, and Y. Kang, Chaos in the NewtonLeipnik system with fractional order, *Chaos, Solitons & Fractals*, **36**(1), 98-103, (2008).

[22] H. Khan, W. F. Alfwzan, J. Alzabut, D. K. Almutairi, M. A. Azim, and R. Thinakaran, Artificial Intelligence And Neural Networking For An Analysis Of Fractal-Fractional Zika Virus Model, *FRACTALS (fractals)*, **33**(08), 1-18, (2025).

[23] S. Abdal, M. F. Tabassumb, and A. Shahzad, Hybrid Fractional Operator for Epidemic Model analysis and application, *Journal of Mathematical Modeling and Fractional Calculus*, **1**(1), 25-37, (2024).

[24] B. Lavenda, G. Nicolis, and M. Herschkowitz-Kaufman, Chemical instabilities and relaxation oscillations, *Journal of Theoretical Biology*, **32**(2), 283-292, (1971).

[25] R. Lefever, G. Nicolis, Chemical instabilities and sustained oscillations, *Journal of theoretical Biology*, **30**(2), 267-284. (1971).

[26] Sing, M. M. Rashidi, D. Kumar, R. Swroop, A fractional model of a dynamical Brusselator reaction-diffusion system arising in triple collision and enzymatic reactions, *Nonlinear Engineering*, **5**(4), 277-285, (2016).

Progr. Fract. Differ. Appl. **12**, No. 1, 115-133 (2026) / www.naturalspublishing.com/Journals.asp

133

[27] I. Bashkirtseva, and L. Ryashko, Sensitivity and chaos control for the forced nonlinear oscillations, *Chaos, Solitons & Fractals*, **26**(5), 1437-1451, (2005).

[28] S. Verma and A. Dwivedi, Integral Transform and Generalized M-Series Fractional Integral Operators, *Journal of Mathematical Modeling and Fractional Calculus*, **2**(1), 1-18, (2025).

[29] S. Sarwar, S. Alkhalaf, S. Iqbal, M. A. Zahid, A note on optimal homotopy asymptotic method for the solutions of fractional order heat-and wave-like partial differential equations. *Computers & Mathematics with Applications*, **70**(5), 942-953, (2015).

[30] S. Sarwar and S. Iqbal, Exact solutions of the non-linear fractional Klein-Gordon equation using the optimal homotopy asymptotic method. *Nonlinear Sci. Lett. A*, **8**(4), 365-373, (2017).

[31] M. Mohammadi, R. Mokhtari and R. Schaback, A meshless method for solving the 2D Brusselator reaction-diffusion system, *Computer Modeling in Engineering & Sciences*, **101**(2), 113-138, (2014).

[32] H. Khan, H. Jafari, R. A. Khan, H. Tajadodi and S. J. Johnston, Numerical Solutions of the Nonlinear Fractional-Order Brusselator System by Bernstein Polynomials, *The Scientific World Journal*, **2014**(1), 257484, (2014).

[33] H. Jafari, A. Kadem and D. Baleanu, Variational Iteration Method for a Fractional-Order Brusselator System, In *Abstract and Applied Analysis (Vol. 2014, No. 1, p. 496323)*. Hindawi Publishing Corporation, (2014).